BRUNGER, A. T., KURIYAN, J. & KARPLUS, M. (1987). *Science*, **235**, 458-460.
COLMAN, P. M. & WEBSTER, R. G. (1985). *Biological Organisation: Macromolecular Interactions at High Resolution.* P&S Biomedical Sciences Symposia.
HUBER, R. (1965). *Acta Cryst.* **19**, 353-356.
KIRKPATRICK, S., GELATT, C. D. JR & VECCHI, M. P. (1983). *Science*, **220**, 671-220.
METROPOLIS, N., ROSENBLUTH, A., ROSENBLUTH, M., TELLER, A. & TELLER, E. (1953). *J. Chem. Phys.* **21**, 1087-1089.
REYNOLDS, R. A., REMINGTON, S. J., WEAVER, L. H., FISHER, R. G., ANDERSON, W. F., AMMON, H. L. & MATTHEWS, B. W. (1985). *Acta Cryst.* **B41**, 139-147.
VAN HEMMEN, J. L. & MORGENSTERN, I. (1983). Editors. *Heidelberg Colloquium on Spin Glasses. Lecture Notes in Physics*, Vol. 192. Berlin: Springer-Verlag.
VAN KAMPEN, N. G. (1981). In *Stochastic Processes in Physics and Chemistry.* Amsterdam: Elsevier.
WEIS, W., BROWN, J. H., CUSACK, S., PAULSON, J. C., SKEHEL, J. J. & WILEY, D. C. (1988). *Nature (London)*, **333**, 426-431.
WILSON, I. A., SKEHEL, J. J. & WILEY, D. C. (1981). *Nature (London)*, **289**, 366-373.

Acta Cryst. (1989). A**45**, 342-346

Observation of Dependent to Independent Bloch Wave Transition in Kikuchi Patterns

BY A. G. WRIGHT AND D. M. BIRD

School of Physics, University of Bath, Bath BA2 7AY, England

(*Received* 4 *October* 1988; *accepted* 16 *January* 1989)

Abstract

The transition from dependent to independent Bloch waves in high-energy electron diffraction theory is demonstrated by observing the disappearance of subsidiary fringes in Kikuchi patterns as the crystal thickness is increased. Comparison is made between experimental and computed Kikuchi band profiles in Si. It is shown that the subsidiary fringes provide a method for thickness determination in zone axis convergent-beam electron diffraction patterns from relatively thin crystals.

1. Introduction

Electron channelling effects have been observed in a wide range of electron microanalytical techniques including X-ray emission (*e.g.* Cherns, Howie & Jacobs, 1973; Taftø & Spence, 1982), energy loss spectroscopy (*e.g.* Taftø & Krivanek, 1982; Taftø, 1987), backscattering (Hagemann & Reimer, 1979), secondary electron emission (Reimer, Badde, Seidel & Buhring, 1971), cathodoluminescence (Pennycook & Howie, 1980), Compton scattering (Williams & Bourdillon, 1982) and thermal diffuse scattering (Rossouw & Bursill, 1985). The feature common to all these is that the interaction between the fast electrons and the crystal is *localized* about the atomic sites $\mathbf{r}_\kappa$. The magnitude of the interaction therefore depends on the electron density at the atoms $[n(\mathbf{r}_\kappa)]$, and it is the variation of this quantity with orientation that gives rise to the channelling effects. In principle, the electron density must be calculated by taking the modulus squared of the wavefunction, which consists of a sum of Bloch states $\psi^{(j)}(\mathbf{r}_\kappa)$ with amplitudes $\varepsilon^{(j)}$:

$$n(\mathbf{r}_\kappa) = \left| \sum_j \varepsilon^{(j)} \psi^{(j)}(\mathbf{r}_\kappa) \right|^2. \quad (1)$$

$n(\mathbf{r}_\kappa)$ therefore contains cross terms between different Bloch states; in other words, (1) represents a *dependent*-Bloch-wave result. It is well known, however, that in thicker crystals the effects of the cross terms diminish owing to summation over all the atoms in the crystal (*i.e.* thickness integration). The electron density is then well represented by the independent-Bloch-wave result [for a full discussion see, for example, Bird & Wright (1989)]

$$n(\mathbf{r}_\kappa) = \sum_j |\varepsilon^{(j)} \psi^{(j)}(\mathbf{r}_\kappa)|^2. \quad (2)$$

In this paper we show that the subsidiary fringes which are observed in Kikuchi bands are a dependent-Bloch-wave phenomenon, and that their disappearance with increasing thickness provides a simple and clear demonstration of the transition to independent waves. The word 'transition' is a little misleading here, but we use it because it has appeared widely in the literature. In fact, the dependent-Bloch-wave result is always correct; the independent-Bloch-wave treatment simply becomes an increasingly good approximation as thickness increases. We also show that the subsidiary fringes may be used to provide an estimate of thickness in zone axis convergent-beam patterns (CBPs) from relatively thin crystals. The occurrence of these fringes has been known for some time (Uyeda, Fukano & Ichinokawa 1954), together with their theoretical explanation (*e.g.* Fujimoto &

0108-7673/89/050342-05$03.00

Kainuma, 1963; Rossouw & Bursill, 1986) but a full thickness sequence has not been previously reported.

2. Experimental and computation

⟨111⟩ Si wafers were chemically thinned to electron transparency. CBPs were taken at room temperature down the [111] zone axis at 200 keV with a JEOL 2000FX electron microscope. Patterns were taken from areas with thicknesses varying from 40 to 400 nm. Parts of the Kikuchi pattern, across the $2\bar{2}0$ and $22\bar{4}$ bands (see Fig. 1), are shown in Figs. 2(*a*)-(*e*) and Figs. 3(*a*)-(*e*) respectively. Subsidiary fringes are observed on both bands. At 60 nm strong fringes are observed right across the $2\bar{2}0$ band, while they are already quite weak near $22\bar{4}$ and almost invisible near $44\bar{8}$. At 100 and 125 nm there are still strong fringes about $2\bar{2}0$, but they have nearly vanished for $4\bar{4}0$ and $6\bar{6}0$. The $22\bar{4}$ fringes are becoming finer and weaker. $2\bar{2}0$ fringes are still clearly visible at 250 nm, but have virtually disappeared at 300 nm. The $22\bar{4}$ fringes have already gone at 250 nm.

Using single scattering theory, the intensity of the Kikuchi pattern in a direction $\mathbf{K}'$ is given by (*e.g.* Rossouw & Bursill, 1986; Bird & Wright, 1989)

$$I(\mathbf{K}') \propto t \sum_{ff'} \sum_{\mathbf{hh}'} C_{\mathbf{0}}^{f}(\mathbf{K}') C_{\mathbf{h}}^{f*}(\mathbf{K}') C_{\mathbf{0}}^{f'*}(\mathbf{K}') C_{\mathbf{h}'}^{f'}(\mathbf{K}') \times \exp(i\Delta^{ff'}t/2)[\sin(\Delta^{ff'}t/2)/(\Delta^{ff'}t/2)] \times \sum_{\kappa} \exp[i(\mathbf{h}'-\mathbf{h}).\mathbf{r}_{\kappa}] S_{\mathbf{h},\mathbf{h}'}^{(\kappa)}(\mathbf{q}). \quad (3)$$

The f, f' sums are over branches of the dispersion surface and the $\mathbf{h}$ and $\mathbf{h}'$ sums are over reciprocal-lattice vectors. The $C_{\mathbf{h}}^{f}$ are Bloch-wave coefficients and t is the crystal thickness. $\Delta^{ff'}(=k_z^f - k_z^{f'})$ is the difference between the z components (perpendicular to the crystal surfaces) of the Bloch wave vectors and is related to the extinction distance $\xi^{ff'}$ by $\Delta^{ff'} = 2\pi/\xi^{ff'}$. The summation over κ is over all atoms in the unit cell and

$$S_{\mathbf{h},\mathbf{h}'}^{(\kappa)}(\mathbf{q}) = v_{\kappa}(\mathbf{q}+\mathbf{h}) v_{\kappa}(\mathbf{q}+\mathbf{h}') (\exp[-M_{\kappa}(\mathbf{h}-\mathbf{h}')^2] - \exp\{-M_{\kappa}[(\mathbf{q}+\mathbf{h})^2 + (\mathbf{q}+\mathbf{h}')^2]\}) \quad (4)$$

describes the thermal diffuse scattering within the Einstein model of lattice vibrations. $\mathbf{q}$ is the scattering vector, $v_{\kappa}(\mathbf{q})$ is the atomic form factor and M_{κ} is the Debye-Waller factor. The incident electron orientation appears in (3) only through $\mathbf{q}$. The initial state is assumed to be a plane wave, but this is not important for the Kikuchi line profile which is controlled by diffraction of the outgoing waves (*e.g.* Bird & Wright, 1989). That is, the details of $S(\mathbf{q})$ are relatively unimportant in (3); what matters are the $C^{f}(\mathbf{K}')$ and $\Delta^{ff'}$.

Nine-beam systematic row calculations have been carried out for the $(2\bar{2}0)$ and $(22\bar{4})$ rows of Si, for orientations $\mathbf{K}'$ as shown in Fig. 1. The incident beam is parallel to the [111] zone axis. Although we consider only one incident orientation this should provide a good approximation in the case of an on-axis CBP because two orientations which are symmetrically disposed on either side of the centre of a band give rise to a Kikuchi pattern similar to that from a single orientation at the band centre (Bird & Wright, 1989). Doyle & Turner (1968) parameters were used to calculate the form factors and the Debye-Waller factor was set at 0·45 Å^2 (Vincent & Bird, 1986). The crystal thickness was first estimated from the subsidiary fringes spacing using two-beam theory (see following section) and then refined by comparing many-beam calculations with experiment. The calculated profiles [with the linear factor t in (3) omitted] are shown in Figs. 2(*f*)-(*j*) and 3(*f*)-(*j*). There is excellent agreement between theory and experiment.

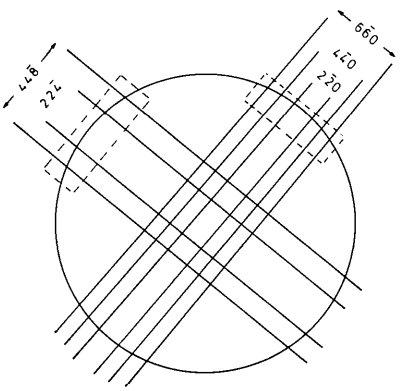

Fig. 1. Schematic diagram of [111] convergent-beam pattern. The circle is the first-order Laue zone and the boxes show the regions of the patterns displayed in Figs. 2 and 3. (Some are from the 60 or 180° rotated bands, but this does not affect the Kikuchi band profile.)

3. Discussion

The thickness-dependent Kikuchi band fringes observed in Figs. 2 and 3 are basically controlled by the $\sin(\Delta t/2)/(\Delta t/2)$ term in (3). As the thickness exceeds the effective extinction distance this term becomes small for $f \neq f'$, but remains unity for $f = f'$. The observation of fringes therefore implies the existence of interference between different Bloch states (*i.e.* dependent waves), while in thicker crystals only terms with $f = f'$ are significant, leading to an independent-Bloch-wave result. It follows that the disappearance of the fringes with increasing thickness provides a direct visualization of the dependent to independent Bloch wave transition. This is particularly clear in the computed profiles in Figs. 2 and 3. As the thickness increases the profiles converge to a given shape; at lower t this overall shape is retained, but is modulated by interference fringes. The sequence in which the fringes disappear in Si is readily

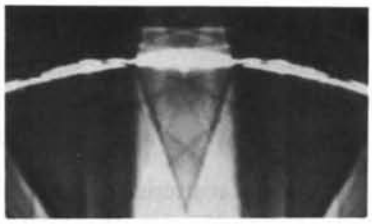

(*a*)

(*b*)

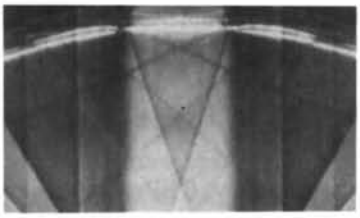

(*c*)

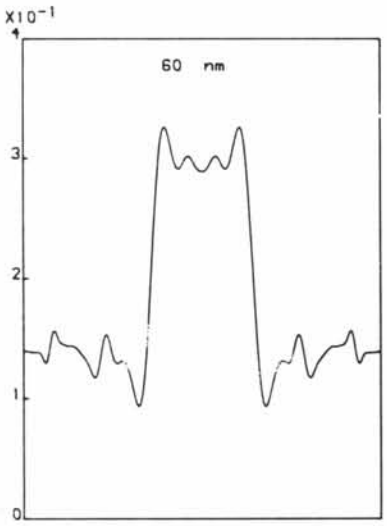

(*f*)

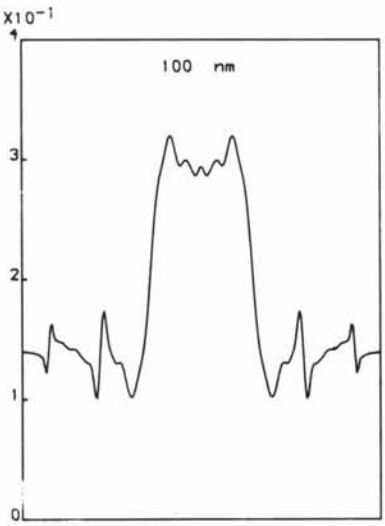

(*g*)

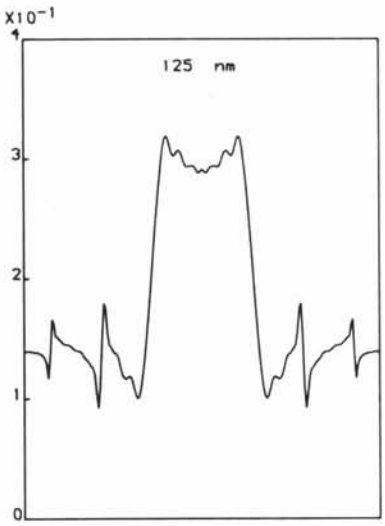

(*h*)

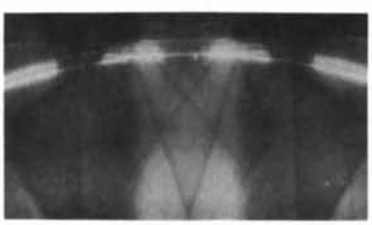

(*d*)

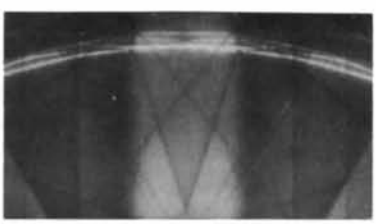

(*e*)

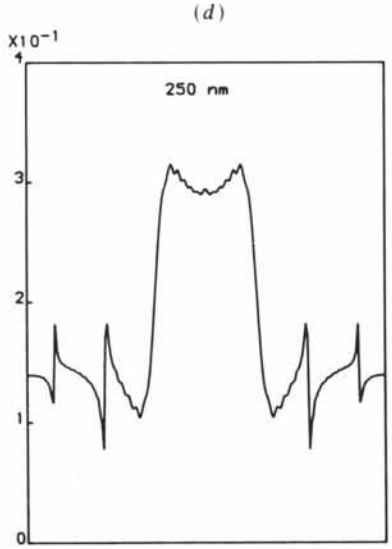

(*i*)

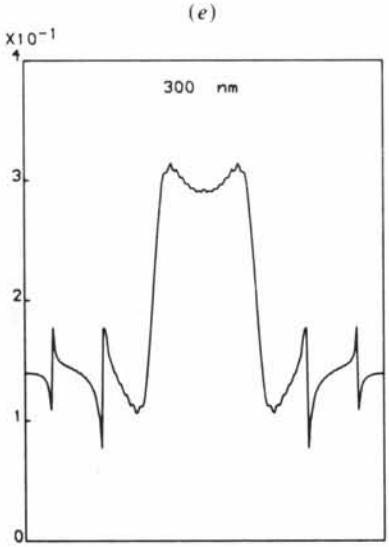

(*j*)

Fig. 2. Experimental (*a*)-(*e*) and theoretical (*f*-*j*) Kikuchi band profiles across the $2\bar{2}0$ band in Si at various crystal thicknesses. The orientation scanned is shown by the dashed box in Fig. 1. See text for details.

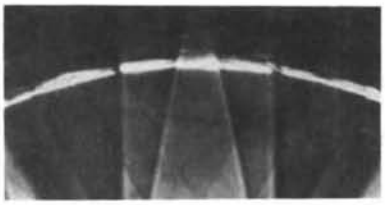

(a)

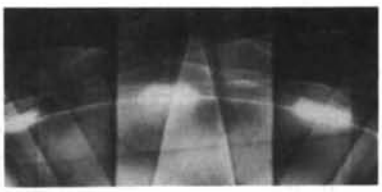

(b)

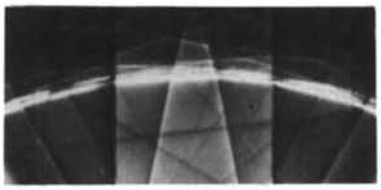

(c)

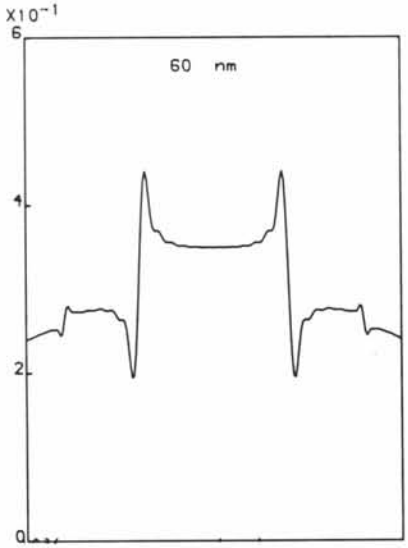

(f)

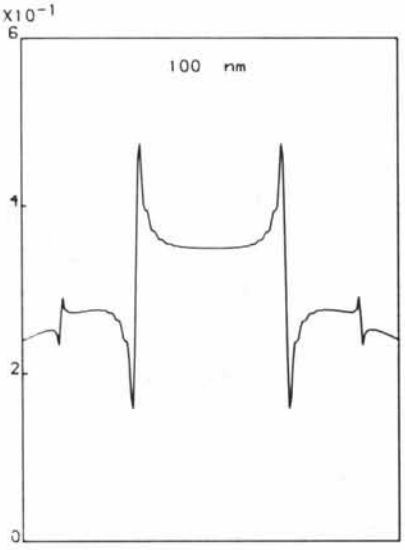

(g)

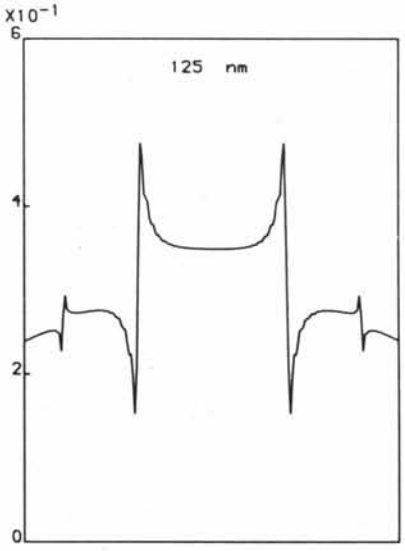

(h)

(d)

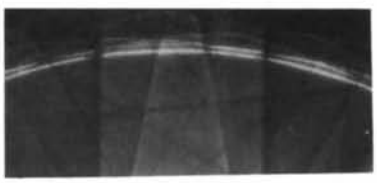

(e)

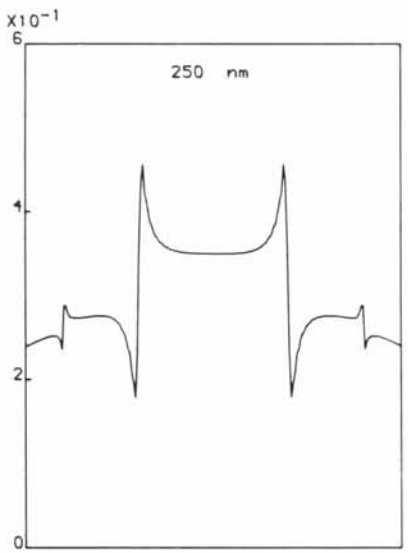

(i)

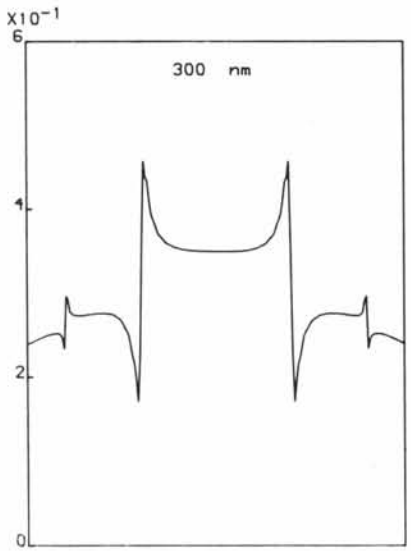

(j)

Fig. 3. As in Fig. 2, but for the $22\bar{4}$ band.

understood. In two-beam theory, the larger the **g** vector, the more rapid is the splitting of the two branches away from the Bragg condition. Therefore, although the extinction distance at the exact Bragg condition increases for larger **g**, the effective extinction distance (*i.e.* the reciprocal of the branch spacing) tends to decrease. In Figs. 2 and 3 the fringes are observed away from the Bragg condition, so it is the effective extinction distance which matters. It follows that the fringes should disappear inversely to the length of the relevant **g** vector, which is exactly as observed. Although absorption has not been included in our calculations, this cannot be responsible for the weakening of the fringes. Only anomalous absorption could be significant, and in two-beam theory the effects of this diminish as we move away from the Bragg condition and the effective extinction distance increases (*e.g.* Hirsch, Howie, Nicholson, Pashley & Whelan, 1977). For a given thickness we would therefore expect a more significant effect for the stronger reflections. In our case the reduction in fringe visibility acts in the opposite direction.

It is clear from the experimental patterns and computed profiles that two-beam theory should provide a good approximation near the weaker Kikuchi lines. In the two-beam limit, and with the incident beam on axis with respect to the Kikuchi band, the orientation-dependent part of (3) can be written (Bird & Wright, 1989)

$$\frac{UW}{U^2+W^2}\left[1-\frac{\sin(\Delta t)}{\Delta t}\right] \quad \text{with} \quad \Delta=(U^2+W^2)^{1/2}/k. \tag{5}$$

U is the magnitude of the structure factor of the given reflection **H**, W the deviation parameter $\mathbf{H}.\delta\mathbf{K}'$ (where $\delta\mathbf{K}'$ is zero at the Bragg condition) and k the fast-electron wave vector. The weak (and smooth) orientation dependence of S has been ignored in (5), together with another oscillatory term which exists for non-centrosymmetric crystals (Bird & Wright, 1989). When $W \gg U$, (5) implies that the fringe spacing $\Delta K'$ corresponds to a change of 2π in Wt/k, so

$$\Delta K'=2\pi k/Ht \text{ or } t=(2\pi k/H^2)(H/\Delta K'). \tag{6}$$

It follows that the subsidiary fringe spacing may be used to determine thickness in a zone axis CBP. The use of this method makes it unnecessary to tilt away to perform a standard two-beam thickness measurement (Kelly, Jostons, Blake & Napier, 1975) and avoids the possibility that the probe moves across the specimen. In fact, the orientation dependence of (5) is similar to that in elastic two-beam theory, so the use of Kikuchi-band fringes is closely analogous to the usual method for thickness determination. There, the $W \gg U$ approximation is not made, but as fewer fringes are observable in Kikuchi patterns the method cannot be as accurate and we suggest that the simpler formula (6) should be used.

To demonstrate the method we look at the $22\bar{4}$ band in Fig. 3(*c*). Here the $2\pi k/H^2$ factor in (6) equals 4·88 nm. From the spacing of the bright fringes we obtain $\Delta K'/H = 0{\cdot}04$ and a thickness of 126 nm. Similarly, in Fig. 2(*d*), the $2\bar{2}0$ fringes have a spacing $\Delta K'/H = 0{\cdot}06$, giving $t = 230$ nm. Values for the thickness obtained in this way from the other patterns in Figs. 2 and 3 also agree well with fits to the many-beam profiles. The most accurate results should be obtained with relatively weak bands, where two-beam theory works best and where the $W \gg U$ condition is more easily satisfied. The sensitivity of the fringes to thickness can be seen in Figs. 2(*b*) and (*c*) where the relatively small thickness difference produces significant changes in the Kikuchi band profile. By using a combination of the bands visible in a pattern we estimate that t may be obtained to an accuracy better than ±10 nm.

This work is supported by the SERC. We thank the Bath University Electron Optics Unit for technical assistance.

References

BIRD, D. M. & WRIGHT, A. G. (1989). *Acta Cryst.* A**45**, 104-109.

CHERNS, D., HOWIE, A. & JACOBS, M. H. (1973). *Z. Naturforsch. Teil A*, **28**, 565-571.

DOYLE, P. A. & TURNER, P. S. (1968). *Acta Cryst.* A**24**, 390-397.

FUJIMOTO, F. & KAINUMA, Y. (1963). *J. Phys. Soc. Jpn*, **18**, 1792-1804.

HAGEMANN, P. & REIMER, L. (1979). *Philos. Mag.* A**40**, 367-375.

HIRSCH, P. B., HOWIE, A., NICHOLSON, R. B., PASHLEY, D. W. & WHELAN, M. J. (1977). *Electron Microscopy of Thin Crystals.* New York: Krieger.

KELLY, P. M., JOSTONS, A., BLAKE, R. G. & NAPIER, J. G. (1975). *Phys. Status Solidi A*, **31**, 771-781.

PENNYCOOK, S. J. & HOWIE, A. (1980). *Philos. Mag.* A**41**, 809-827.

REIMER, L., BADDE, H. G., SEIDEL, H. & BUHRING, W. (1971). *Z. Angew. Phys.* **31**, 145-151.

ROSSOUW, C. J. & BURSILL, L. A. (1985). *Acta Cryst.* B**41**, 248-254.

ROSSOUW, C. J. & BURSILL, L. A. (1986). *Proc. R. Soc. London Ser. A*, **408**, 149-164.

TAFTØ, J. (1987). *Acta Cryst.* A**43**, 208-211.

TAFTØ, J. & KRIVANEK, O. L. (1982). *Nucl. Instrum. Methods*, **194**, 153-158.

TAFTØ, J. & SPENCE, J. C. H. (1982). *Ultramicroscopy*, **9**, 243-248.

UYEDA, R., FUKANO, Y. & ICHINOKAWA, T. (1954). *Acta Cryst.* **7**, 217-218.

VINCENT, R. & BIRD, D. M. (1986). *Philos. Mag.* A**53**, L35-40.

WILLIAMS, B. G. & BOURDILLON, A. J. (1982). *J. Phys. C*, **15**, 6881-6890.